Monatshefte für Chemie 137, 319–337 (2006)
DOI 10.1007/s00706-005-0433-5

Monatshefte für Chemie
Chemical Monthly
Printed in Austria

Amide–Amide Hydrogen Bonding. Semirubin Amides

Nicholas T. Salzameda and **David A. Lightner***

Department of Chemistry, University of Nevada, Reno, Nevada 89557-0020

Received July 1, 2005; accepted August 2, 2005
Published online February 27, 2006

Summary. Semirubins are analogs for one-half of the bilirubin structure and capable of intramolecular hydrogen bonding. Semirubin amides of ammonia and primary amines are also capable of intramolecular hydrogen bonding. From a combination of spectroscopic methods (^{1}H NMR, N*O*E, and VPO), the primary amide is found to engage very effectively in intramolecular hydrogen bonding. The secondary and tertiary amides engage in both intramolecular (*i*) and intermolecular (*ii*) hydrogen bonding: *N*-methyl (*i*, monomer + *ii*, dimer), *N-tert*-butyl (*ii*, dimer), *N*,*N*-diethyl (*i*, monomer + *ii*, dimer). With an oxo-group at C(10), all of the amides are monomeric and most engage in intramolecular hydrogen bonding.

Keywords. Pyrrole; Conformational analysis; NMR; VPO; X-Ray.

Introduction

Semirubins (Fig. 1A) [1, 2] were designed as dipyrrole analogs of the linear tetrapyrrolic natural product, bilirubin [3], the cytotoxic pigment of jaundice [4] (Fig. 1B). Bilirubin folds up into a conformation (called ''ridge-tile,'' Fig. 1C) that is greatly stabilized by intramolecular hydrogen bonding between its dipyrrinone and propionic acid components [5, 6]. The ridge-tile conformation persists even when the propionic acids are ionized [7] but not when esterified – where intermolecularly hydrogen-bonded (dipyrrinone to dipyrrinone) dimers prevail [3, 8, 9]. Like bilirubin, semirubins with 6-carbon (or even longer) alkanoic acid chains engage in intramolecular hydrogen bonding and are monomeric in nonpolar solvents like $CHCl_3$ [1]. Their esters, in contrast, are dimeric, held together by intermolecular hydrogen bonding. 10-Oxosemirubins, which are dipyrrole models for 10-oxobilirubin (thought to be important in non-conjugate-dependent, alternate pathways for pigment elimination [10, 11]) also form intramolecular hydrogen bonds. Unlike semirubin esters, the 10-oxoesters probably do not engage in hydrogen bonding and remain monomers in solution [1].

* Corresponding author. E-mail: lightner@scs.unr.edu

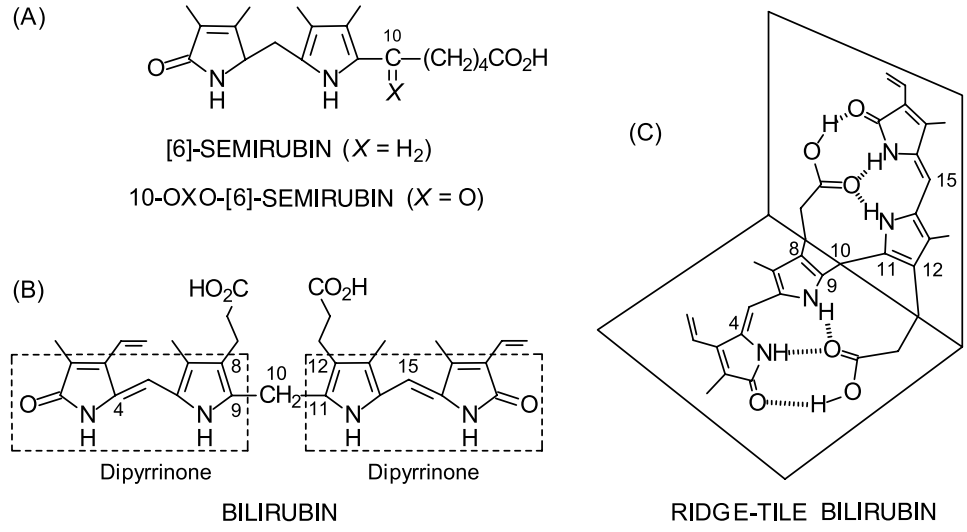

Fig. 1. (A) Semirubin and its 10-oxo analog; we name these [6]-semirubin and 10-oxo-[6]-semirubin, where [6] designates the number of carbon atoms in the acid chain; (B) linear representation of bilirubin; the most stable conformation of bilirubin is not linear but shaped like a ridge tile (C), and stabilized by intramolecular hydrogen bonding

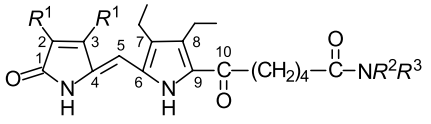

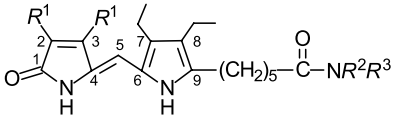

	R^1	R^2	R^3
1:	*Et*	H	H
2:	*Et*	H	*Me*
3:	*Me*	H	*t-Bu*
4:	*Me*	*Et*	*Et*

	R^1	R^2	R^3
5:	*Et*	H	H
6:	*Et*	H	*Me*
7:	*Me*	H	*t-Bu*
8:	*Me*	*Et*	*Et*

Fig. 2. The semirubin amides **5**–**8** and 10-oxosemirubin amides **1**–**4** of this work

The few investigations of bilirubin amides indicate that their primary and secondary amides can and do participate in strong intramolecular hydrogen bonding [12]. Tertiary amides do not particularly [13]. In the following, we describe our investigations of the conformation and hydrogen bonding of semirubin amides **1**–**8** (Fig. 2), of which the primary and secondary amides have the potential for intramolecular hydrogen bonding; whereas, the tertiary amides do not. The addition of a carbonyl at C(10) has a major influence on the acid chain conformation, forcing the 10-oxosemirubins to be monomeric in nonpolar solvents.

Results and Discussion

Synthesis Aspects

All of the amides of this work were prepared in 32–80% yields from the corresponding carboxylic acids and amines using diphenylphosphoryl azide as coupling

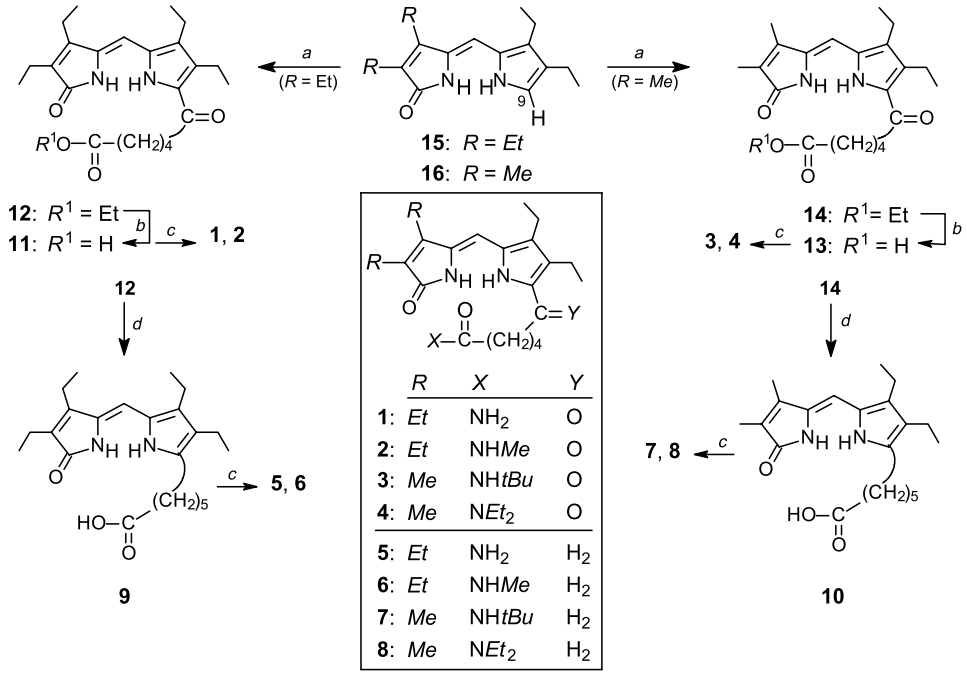

a: $EtO_2C(CH_2)_4COCl$, $AlCl_3$; *b*: NaOH; *c*: diphenylphosphoryl azide + NH_4Cl, $MeNH_2Cl$, $tBuNH_2$, or Et_2NH; *d*: $NaBH_4$

Scheme 1

agent [12–14], as shown in Scheme 1. Semirubin acids **9** and **10** come from 10-oxosemirubin esters **12** and **14** in 66–71% yield by reduction using $NaBH_4$. 10-Oxosemirubin acid precursors (**11** and **13**) to amides **1**–**4** were prepared in 89% yield from the corresponding esters by saponification using 2 *M* NaOH in aq. *THF*. The 10-oxosemirubin esters were prepared from the known 9*H*-dipyrrinones **15** [15] and **16** [16] and the half-ester acid chloride of adipic acid in 60–70% yield by *Friedel-Crafts* acylations catalyzed by anhydrous $AlCl_3$ [1].

Constitutional Structure

The constitutional structures of **1**–**8** follow from the known dipyrrinones **15** and **16** [15, 16], the method of synthesis, and ^{13}C NMR spectra (Table 1). After allowing for the different substituents (methyl, ethyl) on the pyrrolinone ring, the ^{13}C NMR spectra of the carbon skeletons of **1**–**4** are very similar, as are the ^{13}C NMR data for **5**–**8**. The main differences observed are those associated with the presence or absence of the 10-oxo group and the N-substituents of the amides.

Molecularity in Solution from VPO Measurements

Vapor pressure osmometry (VPO) has been used effectively to learn that bilirubin esters tend to form dimers [3, 8, 9], whereas bilirubin acids and their carboxylate anions are monomeric [9] in solvents such as chloroform or *THF*. There are no data on the molecularity of 10-oxobilirubins in solution. Although there are no similar

Table 1. Comparison of ^{13}C NMR chemical shift assignments for 10-oxo-[6]-semirubin amides **1**–**4** and [6]-semirubin amides **5**–**8** in $(CD_3)_2SO$; chemical shifts in δ (ppm) downfield from $(CH_3)_4Si$

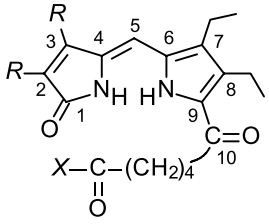

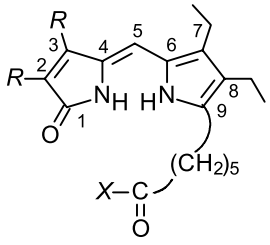

Position	**1**	**2**	**3**	**4**	**5**	**6**	**7**	**8**
1-CO	172.3	172.3	171.6	170.8	171.6	171.5	171.6	170.9
2	134.0	134.0	135.4	135.4	121.1	126.9	121.0	121.0
3	146.9	146.9	141.7	141.7	146.7	146.7	141.3	141.3
4	129.5	129.6	127.6	127.6	128.4	128.4	128.8	128.8
5	96.0	96.0	95.8	95.8	97.7	97.7	97.6	97.6
6	132.0	132.0	132.0	132.0	126.9	121.1	123.4	123.4
7	131.7	131.7	128.8	128.9	128.9	128.9	128.5	128.5
8	127.6	127.6	126.7	126.7	133.8	133.7	133.6	133.6
9	128.8	128.8	129.5	129.6	120.8	120.8	120.7	120.8
10-CO	189.7	189.7	189.7	189.8	25.5	25.4	25.5	25.5
11-CH_2	38.3	38.3	38.4	38.4	24.9	25.1	25.3	24.8
12-CH_2	24.9	23.6	23.5	23.6	28.6	28.7	28.5	28.7
13-CH_2	23.6	25.1	25.3	24.5	30.1	30.1	30.1	30.1
14-CH_2	35.1	35.3	36.1	32.1	35.0	35.3	36.0	32.0
15-CO	174.2	172.4	172.7	172.7	174.3	172.4	171.9	171.9
2^1 CH_2 or CH_3	16.9	17.0	16.4	16.5	16.7	16.7	16.6	16.6
2^2 CH_2 or CH_3	16.3	16.4	–	–	16.3	16.3	–	–
3^1 CH_2 or CH_3	16.5	16.5	16.5	15.7	17.0	17.1	16.7	17.0
3^2 CH_2 or CH_3	15.7	15.7	–	–	15.7	15.8	–	–
7^1 CH_2CH_3	16.5	16.5	17.9	17.9	17.0	17.1	17.1	17.1
7^2 CH_2CH_3	13.7	13.7	9.5	9.6	13.9	13.9	9.6	9.6
8^1 CH_2CH_3	17.9	17.9	15.7	16.4	17.5	17.1	17.0	16.7
8^2 CH_2CH_3	15.5	15.5	8.4	8.4	16.6	16.6	8.3	8.3

VPO studies reported for bilirubin amides, other spectroscopic measurements such as ^1H NMR and CD [12, 13] are consistent with monomers in chloroform for primary and secondary amides. There have been no studies of 10-oxobilirubin amides.

Earlier, we reported on the molecularity of [6]-semirubin and 10-oxo-[6]-semirubin (Fig. 1A) and their esters in chloroform [1], a study that showed both semirubin and 10-oxosemirubin were monomeric in the concentration range $1.7–6.1\times10^{-3}$ mol kg^{-1}. The methyl ester of the semirubin tended toward dimeric; whereas, the ethyl ester of the 10-oxosemirubin was monomeric. The latter, surprisingly, suggested that the 10-oxo group oriented the ester toward the dipyrrinone NHs, thereby interfering with dimer formation.

As in earlier studies [1, 2], all of the 10-oxo-[6]-semirubin amides of this work (**1**–**4**) are monomeric in $CHCl_3$. In contrast, semirubin secondary and tertiary

amides (**6**–**8**) without the 10-oxo substituent are dimeric or a mixture of monomers and dimers (**6**), but the primary amide (**5**) is monomeric. Interestingly, even when a bulky *N-tert*-butyl group might interfere with intramolecular hydrogen bonding, the 10-oxo-[6]-semirubin amide (**3**) is monomeric. The 10-oxo substituent apparently orients the acid chain toward the dipyrrinone hydrogen bonding region, thereby effectively blocking dimerization that would occur *via* intermolecular hydrogen bonding.

Beer's Law and Aggregation

To explore the possibility of aggregation in chloroform solution, we examined how well **1**–**8** fit *Beer's* Law over the range $\sim 1.5\times10^{-6}\,M$ to $1.5\times10^{-3}\,M$. Consistent

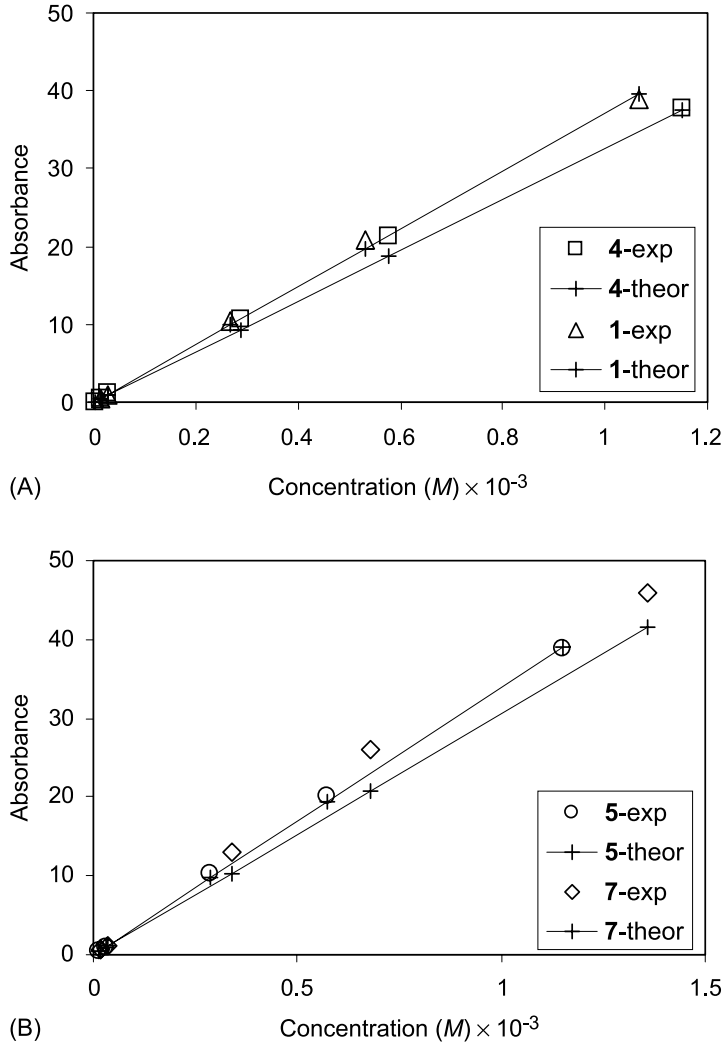

Fig. 3. *Beer's* Law plots of absorbance *vs*. concentration in $CHCl_3$ for (A) 10-oxosemirubin amide **1** (△, +) and 10-oxosemirubin *N*,*N*-diethylamide **4** (□, +) and (B) semirubin amide **5** (○, +) and semirubin *N-tert*-butylamide **7** (◇, +)

Table 2. Molecular weights (*MW*s) of 10-oxo-[6]-semirubin amides **1**–**4** and [6]-semirubin amides **5**–**8** determined by vapor pressure osmometry[a] at 45°C in $CHCl_3$ solution,[b] and *Beer's* Law behavior in $CHCl_3$

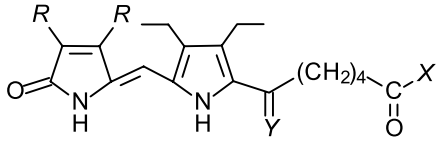

Amide	*R*	*X*	*Y*	Formula weight (*FW*, g mol^{-1})	Measured *MW* (g mol^{-1})	*Beer's* Law[c]
1	*Et*	NH_2	O	399	400 ± 17	ND
2	*Et*	NH*Me*	O	413	425 ± 9	ND
3	*Me*	NH*tBu*	O	427	433 ± 15	ND
4	*Me*	NEt_2	O	427	420 ± 4	ND
5	*Et*	NH_2	H_2	385	390 ± 3	ND
6	*Et*	NH*Me*	H_2	399	600 ± 7	D
7	*Me*	NH*tBu*	H_2	413	817 ± 20	D
8	*Me*	NEt_2	H_2	413	619 ± 20	D

[a] Calibrated with benzil ($FW = 210$ g mol^{-1}, $MW = 220 \pm 15$ g mol^{-1}); [b] conc. range, 1.4–5.1×10^{-3} mol kg^{-1}; [c] D = deviation, ND = no deviation from *Beer's* Law

with the data from VPO measurements, *Beer's* Law plots show no deviation for **1**–**5**, but for *N*-methylamide **6**, *N*-*tert*-butylamide **7**, and *N*,*N*-diethylamide **8**, deviations are clearly evident (Fig. 3). These data, summarized in Table 2 are consistent with a monomer ⇄ dimer equilibrium for **7** and **8**, and with monomeric solutions of **1**–**5** over the concentration range used. They are also consistent with our findings for [6]-semirubin methyl ester [1] showing *Beer's* Law deviation and a dimer by VPO. The data for the 10-oxosemirubin amides **1**–**4** (Table 2) are consistent with entirely monomeric solutions and with the earlier observations for the ethyl ester of 10-oxo-[6]-semirubin [1]. Thus, the 10-oxo group exerts a strong influence on preventing dimerization of the *N*,*N*-dimethylamide (**4**) and the *N*-*tert*-butylamide (**3**), presumably by interfering with the intermolecular hydrogen bonding that is evident for **7** and **8**, as shown in the following.

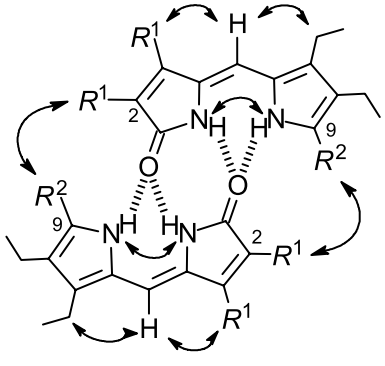

Fig. 4. Dipyrrinone planar dimer secured by intermolecular hydrogen bonding; curved arrows indicate N*O*Es; the N*O*E between R^1 and R^2 is diagnostic of this type of dimer

Hydrogen Bonding Detected by ^1H NMR Spectroscopy

Dipyrrinones are known to be excellent participants in hydrogen bonding, either by self-association [3, 17, 18] or with a carboxyl group [1, 19]. Such hydrogen bonding may be recognized by the pyrrole and lactam N–H chemical shifts in the ^1H NMR spectrum [1, 17–19]. Thus, although a dipyrrinone monomer in $CHCl_3$ might show N–H chemical shifts at ~8 ppm [17], the planar intermolecularly hydrogen-bonded dimer (Fig. 4) would show strongly deshielded lactam and pyrrole N–H chemical shifts, down to ~11 and 10 ppm [17, 18]. Such dimers have been detected in dipyrrinone crystals [3, 20] and in their solutions in $CDCl_3$ by N*O*E measurements [9, 18]. In contrast, when the dipyrrinones serve as receptors to CO_2H groups and bind securely by hydrogen bonding, the N–H chemical shifts are found to be relatively more shielded, particularly the pyrrole N–H (~9 ppm) and to a lesser extent the lactam N–H (~10.5 ppm), whether in inter- [17, 18] or intramolecular [1, 2] hydrogen bonding. In fact, in [6]-semirubin [1], the lactam and pyrrole N–H chemical shifts

Table 3. Comparison of the lactam, pyrrole, and amide NH chemical shifts[a] of 10-oxo-[6]-semirubin amides **1**–**4** and [6]-semirubin amides **5**–**8** in $CDCl_3$ and $(CD_3)_2SO$ solvents

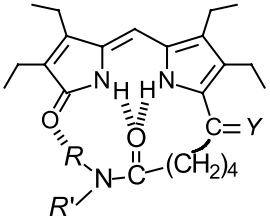

	Pigments			$CDCl_3$				$(CD_3)_2SO$			
				Lactam NH	Pyrrole NH	Amide NH		Lactam NH	Pyrrole NH	Amide NH	
	R	*R′*	*Y*			*syn*	*anti*			*syn*	*anti*
1	H	H	O	11.57	10.28	8.52	5.82	10.67	10.39	7.27	6.71
2	H	*Me*		11.85	10.36	8.62	–	10.60	10.33	7.67	
	Me	H	O	(9.94)	(10.6)	–	6.11				
3	*tBu*	H	O	9.68	9.00	–	5.47	10.60	10.38	7.35	
4	*Et*	*Et*	O	10.04	9.59	–	–	10.6	10.4	–	
5	H	H	H_2	10.87	9.81	8.94	5.56	9.87	10.15	7.22	6.67
6	H	*Me*	H_2	11.26	10.10	8.92	–				
	Me	H	H_2	9.99	10.89	–	5.52	9.84	10.14	7.67	
7	*tBu*	H	H_2	11.32	10.18	–	5.19	9.84	10.10	7.3	
8	*Et*	*Et*	H_2	11.03	10.10	–	–	9.84	10.10	–	
β,β'-Dimethyl *MBR*				10.68	9.04	–		9.85	10.10	–	
diamide				10.77	9.88	8.91	5.55	9.90	10.94	8.24	8.22
bis-*N*-methylamide				11.04	10.13	8.92		10.05	10.25	8.30	
bis-*N*,*N*-dimethylamide				10.78	9.61	–		9.70	10.35	–	
methyl ester				10.06	9.93	–		9.77	10.19	–	

[a] δ, in ppm downfield from $(CH_3)_4Si$

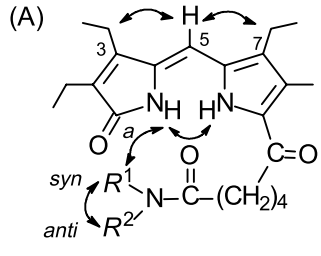

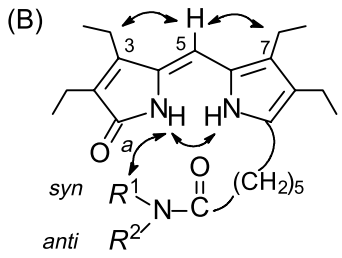

		NOE[a]			NOE[a]
1:	$R^1 = R^2 = H$	✓	**5**:	$R^1 = R^2 = H$	✓
2:	$R^1 = H, R^2 = Me$	✓	**6**:	$R^1 = H, R^2 = Me$	✓
	$R^1 = Me, R^2 = H$	✓		$R^1 = Me, R^2 = H$	X
3:	$R^1 = H, R^2 = tBu$	X	**7**:	$R^1 = H, R^2 = tBu$	X
				$R^1 = tBu, R^2 = H$	X
4:	$R^1 = R^2 = Et$	✓	**8**:	$R^1 = R^2 = Et$	X

Fig. 5. Intramolecularly hydrogen bonded conformations and their NOEs (shown by curved arrows); a: ✓ = NOE observed and X = NOE not observed between R^1 and the lactam NH

(10.48 and 8.98) in $CDCl_3$ are very similar to those found in bilirubin (~10.6 and ~9.2). Similarly, the same N–H chemical shifts from 10-oxo-[6]-semirubin (10.66 and 9.21) [1] may be taken as an indication of intramolecular hydrogen bonding.

Similarly, by examining the N–H chemical shifts of amides **1**–**8**, one can learn whether the compounds engage in hydrogen bonding, whether intra- or intermolecular. Their N–H chemical shift data (Table 3) reveals strongly deshielded (~8.5 ppm) and shielded (~5.8 ppm) hydrogens of the amide NH_2, characteristic of a conformation (Fig. 5A) where in **1** and **4** the *syn* N–H (R^1) is involved in intramolecular hydrogen bonding and is thus considerably more deshielded than the *anti*. Their amide NH_2 chemical shifts are thus nicely comparable to those seen in a bilirubin diamide (Table 3) where intramolecular hydrogen bonding was deduced. These findings are consistent with the VPO data, which show monomers, and they indicate hydrogen-bonded monomers as in Fig. 5.

At the other extreme, where amide to dipyrrinone hydrogen bonding might not be expected, *N*,*N*-diethylamide **8** exhibits lactam and pyrrole NH chemical shifts characteristic of an intermolecularly hydrogen-bonded planar dimer in **8** (Fig. 4), but **4** exhibits a more shielded (by ~1 ppm) lactam NH, which we take as an indication that **4** is not dimeric, but may have a structure akin to that of Fig. 5A. These findings are consistent with the VPO findings that **4** is monomeric and **8** tends toward dimeric.

N-Methylamides **2** and **6** and *N-tert*-butylamides **3** and **7** differ from those above. All are capable of intramolecular hydrogen bonding (Fig. 5). The *N-tert*-butylamides **3** and **7** clearly do not show an amide N–H chemical shift corresponding to a hydrogen-bonded amide (Table 3). Rather, the 5.47 (**3**) and 5.19 (**7**) N–H chemical shifts are characteristic of an *anti* N–H that cannot engage in intramolecular hydrogen bonding. The strong preference for an amide conformation

($\sim$6 kJ mol^{-1}) with a *syn-N-tert*-butyl group eclipsing the amide carbonyl apparently is sufficiently stable to overcome the potential benefits of N–H $\cdots$ O intramolecular hydrogen bonding that might occur in the *anti-N-tert*-butyl. In contrast, *N*-methylamide **2** shows both *syn* and *anti* amide conformers: (*i*) an intramolecularly hydrogen-bonded *syn-N*-methyl isomer (favored over *anti* by $\sim$4 kJ mol^{-1}) with the *anti* N–H is strongly shielded and not involved in *intra*molecular hydrogen bonding, and (*ii*) an intramolecularly hydrogen-bonded *anti N*-methyl conformer, where the *syn* N–H is strongly deshielded due to intramolecular hydrogen bonding (as in **1** and **5**). The lactam and pyrrole N–H chemical shifts of **2** correlate well with those of **1** (for intramolecular hydrogen bonding), and **4** (for weaker intramolecular hydrogen bonding but still monomeric). *N*-Methylamide **6** also shows both *syn* and *anti* amide isomers; however, we observe intramolecular bonding only in the *anti* isomer. The *syn* isomer exhibits intermolecular hydrogen bonding, as with carboxylic acid esters. In **6**, the lactam and pyrrole chemical shifts correlate well with those of **5** (for intramolecular hydrogen bonding) and **8** (for intermolecular hydrogen bonding). These data, when correlated with the VPO data indicate that **2** and **3** are monomeric and that whereas the *anti*-isomer (of **2**) engages in intramolecular hydrogen bonding, the *syn*-isomers of **2** and **3** engage in partial intramolecular hydrogen bonding and also do not form intermolecular dimers. Similarly, the ^{1}H NMR data from **6** and **7** correlate nicely with their VPO data, which show that **7** is a dimer and **6** is a monomer + dimer mixture.

Nuclear Overhauser Effect and Conformation

Nuclear *Overhauser* Effects (N*O*Es) were found from **1**–**8**, as indicated in Figs. 4 and 5. Thus, all of the dipyrrinones remain in the *syn-Z* conformation, as evidenced by the N*O*Es between (i) the C_5-H and the C_3 and C_7 ethyls and (ii) the lactam and pyrrole N–Hs. In **1** and **2**, N*O*Es are seen between the *syn*-N–H of the amide and the lactam N–H. In **2** and **4** one sees an N*O*E between the lactam NH and the *syn-N*-alkyl. All are monomers, as indicated by VPO, and consistent with an earlier report [18] that the presence of the 10-oxo group orients the alkyl chain terminus toward the dipyrrinone N–Hs. Similarly, in **5** and **6** one finds N*O*Es between the *syn*-amide N–Hs and the lactam N–H. N*O*Es between the C_2 and C_9 alkyl groups, R^1 and R^2 in the planar dimer of Fig. 4 [17], are seen in **7** and **8**.

Molecular Dynamics Calculations

In support of the conclusions reached above from VPO, *Beer's* Law plots, and NMR spectroscopy, molecular dynamics [21] calculations of **1**–**6** indicate a special stability associated with intramolecularly hydrogen-bonded conformations (Fig. 6). The intramolecularly hydrogen-bonded conformations are computed to be some 42 to 46 kJ mol^{-1} lower in energy than the non-hydrogen bonded forms. The intramolecularly hydrogen-bonded amides and N-methylamides (**1**, **2**, **5**, **6**) have computed parameters similar to those found in [6]-semirubin and 10-oxo-[6]-semirubin [1] and to bilirubin amides [12].

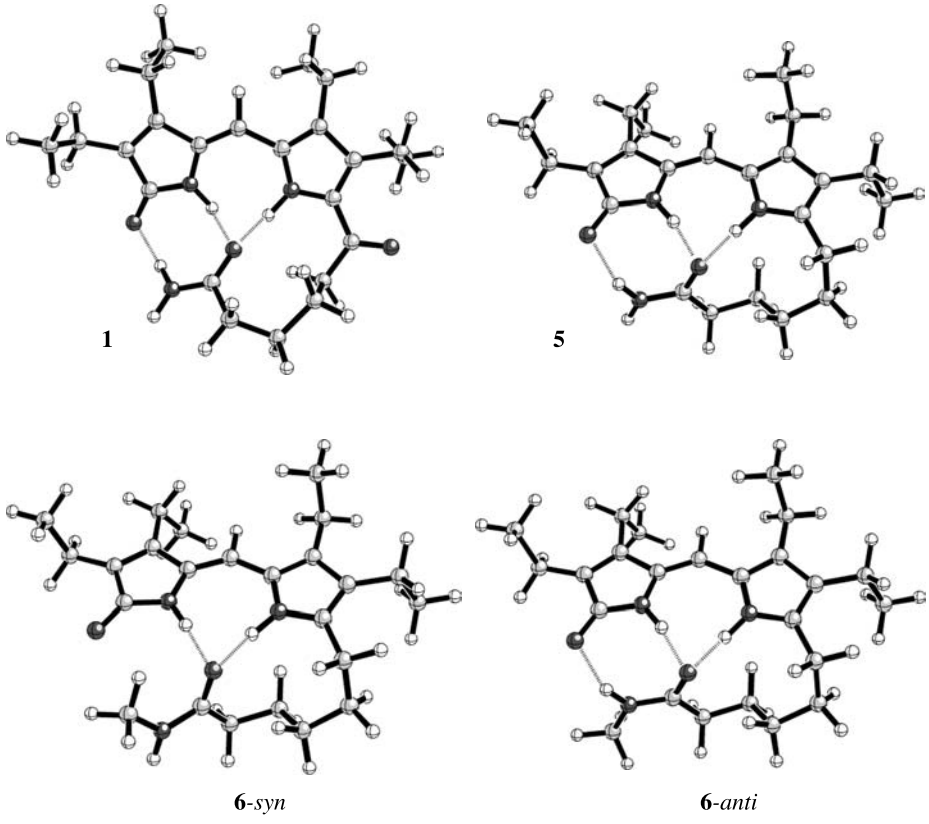

Fig. 6. Ball and Stick [21] drawings of the energy-minimized most-stable conformations of 10-oxo-[6]-semirubin amide **1**, semirubin amide **5**, and the *syn* and *anti* isomers of **6**

The dipyrrinone moiety in **1**, **2**, **5**, and **6** is twisted somewhat, with C(4)–C(5)–C(6)–N torsion angles of approximately 9.3° (**1**); 15.2° (*anti*-**2**), 20.7° (*syn*-**2**); 6.9° (**5**); 5.0° (*syn*-**6**), 8.3° (*anti*-**6**). The C(11)–C(10)–C(9)–N torsion angles are approximately 0.9° (**1**); 0.1° (*anti*-**2**), 9.3° (*syn*-**2**); 79.9° (**5**); 83.4° (*syn*-**6**), 78.8° (*anti*-**6**) as compared to ~60° in mesobilirubin [2]. While molecular dynamics calculations suggest that **5** adopts a dipyrrinone molecular geometry very similar to that found in bilirubin [24], the energetically most favored structure of **1** differs somewhat from that of **5**, presumably because its C(10) carbon is sp^2 hybridized rather than sp^3.

*Crystal Structure and Conformation: 10-Oxo-[6]-N-methylsemirubin amide (**2**)*

An examination of the crystal structure drawings of 10-oxosemirubin *N*-methylamide **2** clearly shows two non-symmetry-equivalent molecules (A and B) in the unit cell, with neither intramolecular hydrogen bonding nor the intermolecular hydrogen bonding seen in other dipyrrinone crystal structures [3, 20]. The dipyrrinones adopt a (*syn*-*Z*) configuration of the C=C at C(4). The observed bond lengths suggest that delocalization over an individual conjugated system of two pyrrole rings is rather limited, since the C(4)=C(5) double bond seems to be an essentially full double bond (average bond length of 1.35 Å). The same bond length is found in the crystal structure of kryptopyrromethenone [20].

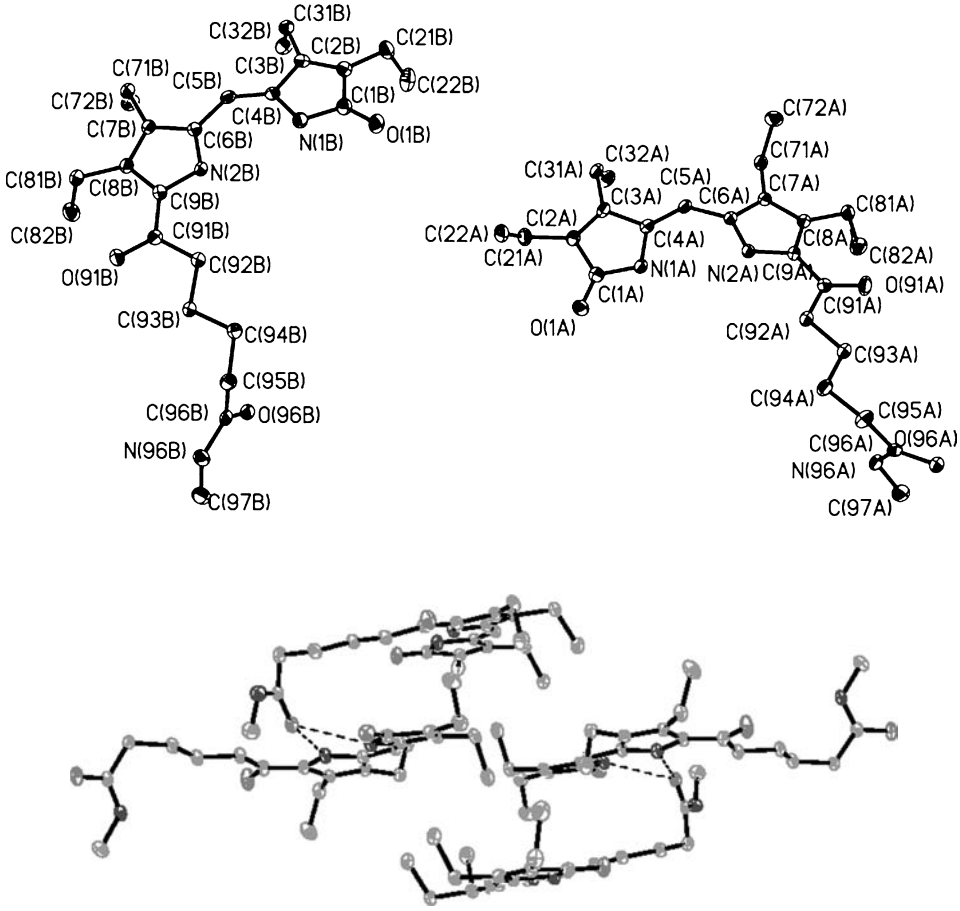

Fig. 7. (Upper) Crystal structure drawing and numbering system of the non-symmetry-equivalent molecules B and A of **2**; hydrogen atoms are removed for clarity of presentation; librational ellipsoids have been drawn with 50% probability; (Lower) crystal stacking pattern of **2** showing intermolecular hydrogen bonding between the dipyrrinone of A and *N*-methylamide carbonyl of B

It has been demonstrated that when the possibility of lactam/lactim tautomerism exists, the lactam form predominates by about 4–10 orders of magnitude over the lactim form for bile pigments in solution and in all known rubin X-ray structures. Consistent with this, **2** is found to prefer the bis-lactam tautomeric form, as confirmed by lactam C=O bond lengths that are comparable to C=O distances in ordinary lactams. The C(1)=O(1) bond length of **2** is 1.231 Å in molecule A and 1.232 Å in molecule B, which compare favorably with that of kryptopyrromethenone (1.216 Å) [20] and bilirubin, where the corresponding bond lengths are 1.25 and 1.28 Å [5c]. Furthermore, the lactam C–N bond distances in **2** are consistent with a carbon nitrogen *single* bond, C(1A)–N(1A) ∼1.378 Å and C(1B)–N(1B) ∼1.368 Å – nearly identical to that of kryptopyrromethenone [20] and very similar to those found in bilirubin [5c, d] (1.41 and 1.35 Å). In contrast, for the lactim (methyl ether) structure, as in 5-ethoxy-5′-ethoxycarbonyl-3′,4′-dihydro-3,4-dimethyl-2,2′-pyrromethane [22], the C=N and C–O(Et) bond distances are 1.28 and 1.33 Å. For bilirubin, the lactam tautomer was proven independently by

Table 4. Solvent-dependence of the *UV*-visible spectral data[a] of 10-oxo-[6]-semirubin amides **1**–**4** and [6]-semirubin amides **5**–**8**

Compound	ε^{max} (λ^{max})				
	Benzene	$CHCl_3$	CH_3OH	CH_3CN	$(CH_3)_2SO$
1	41300 (425)	39000 (425)	29100 (418)	34700 (416)	28200 (419)
	37100 (401)	36600 (402)	32400 (397)	35200 (393)	31000 (397)
2	38900 (422)	32200 (422)	28800 (417)	27600 (412)	28800 (419)
	36800 (399)	33400 (400)	33000 (396)	32200 (390)	31400 (397)
3	30000 (418)	24200 (417)	26700 (414)	23800 (407)	26900 (416)
	30800 (395)	28400 (396)	30700 (394)	29400 (287)	30300 (395)
4	36900 (418)	30800 (419)	26000 (414)	26500 (410)	26000 (417)
	35600 (394)	32500 (396)	30400 (394)	30800 (388)	29100 (395)
5	33000 (427)	33900 (421)	35600 (420)	33400 (414)	33900 (419)
	31700 (412)				
6	33800 (426)	33400 (420)	37900 (420)	34600 (409)	35400 (419)
	33000 (413)				
7	33800 (412)	30500 (411)	36000 (417)	31300 (405)	31300 (416)
8	30000 (415)	29100 (412)	33200 (417)	30000 (405)	31000 (415)

[a] At 25°C in concentrations $2.1–2.7 \times 10^{-5}\,M$, λ^{max} in nm, ε^{max} in $dm^3\,mol^{-1}\,cm^{-1}$; solvents other than $CHCl_3$ contain 2% $CHCl_3$

^{15}N NMR: $\delta_{N(21)} = -249.8$, $\delta_{N(24)} = -249.2$, $\delta_{N(22)} = -231.3$, $\delta_{N(23)} = -231.6$ *vs.* $\delta_N = -140$ ppm for a lactim N [3].

Optical Spectra

The *UV*-visible spectral data for **1**–**8** in solvents with a wide range of polarity are shown in Table 4. The long wavelength bands of the 10-oxosemirubin amides (**1**–**4**) show only a small (2–6 nm) decrease in λ^{max} in going from nonpolar (benzene, $CHCl_3$) solvents to $(CH_3)_2SO$ but larger decreases in methanol (4–5 nm) and acetonitrile (8–11 nm). The ε^{max} values are generally higher in the nonpolar solvent. Similar trends are seen in **5**–**8**, but **7** and **8** show little variation across the range of solvent polarity, except in CH_3CN. Interestingly, **1**, **2**, **5**, and **6** show nearly the same λ^{max} in a given solvent, and λ^{max} tends to be bathochromically shifted from that of **3**, **4**, **7**, and **8** in solvents likely to promote hydrogen bonding. While the spectral shifts do not unambiguously confirm an intramolecularly hydrogen bonded structure for **1**, **2**, **5**, and **6**, they lend support to this conclusion, reached on the basis of NMR spectral analysis and VPO studies, and they are consistent with their ability to adopt a unique conformational structure in nonpolar solvents.

Concluding Comments

Amide to dipyrrinone (amide) intramolecular hydrogen bonding involving the amide N–H and the dipyrrinone amide and pyrrole NHs was observed for primary amide (**5**) and *N*-methylamide (**6**) of the [6]-semirubin motif, which are monomeric

in $CHCl_3$ solution at $\sim 10^{-3}\,M$ concentration. Only the *anti*-conformation of the *N*-methylamide exhibits the full hydrogen bonding; the *syn* only partial. In contrast, the *N-tert*-butylamide and *N*,*N*-diethylamide (**7** and **8**) are dimeric in $CHCl_3$ and engage in intermolecular hydrogen bonding. Remarkably, the 10-oxo-[6]-semirubin analogs (**1**–**4**) are all monomeric in $CHCl_3$ and most engage in intramolecular hydrogen bonding. The 10-oxo group apparently orients itself *anti* to the pyrrole NH, thereby forcing the six-carbon amide chain in the direction of the lactam pyrrole NHs. Possibly due to stacking forces in the crystal of **2**, the *N*-methylamide terminus is extended not to the attached dipyrrinone but to the dipyrrinone unit of a neighboring molecule.

Experimental

Nuclear magnetic resonance (NMR) spectra were obtained in $CDCl_3$ solvent on a GE QE-300 spectrometer operating at 300 MHz (for most of the ^{1}H NMR data, unless otherwise indicated) and at 125 MHz on a Varian Unity Plus 500 MHz spectrometer for most of the ^{13}C NMR data. N*O*E NMR were obtained at 500 MHz. Chemical shifts were reported in δ(ppm) referenced to the residual $CHCl_3$ ^{1}H signal at 7.26 ppm and ^{13}C at 77.23 ppm. Infrared spectra were recorded on a Perkin-Elmer model 1610-*FT IR* instrument. Ultraviolet-visible spectra were recorded on a Perkin-Elmer λ-12 spectrophotometer. Melting points were taken on a Mel-Temp capillary apparatus and are uncorrected. Combustion analyses for C, H, and N were carried out by Desert Analytics, Tucson, AZ, and gave results within $\pm 0.4\%$ of the theoretical values. Analytical thin layer chromatography (TLC) was carried out on J. T. Baker silica gel IB-F plates (125 μm layers). Radial chromatography was carried out on Merck preparative layer grade silica gel PF_{254} with $CaSO_4$ binder using a Chromatotron (Harrison Research, Inc., Palo Alto, CA) with 1, 2, or 4 mm thick rotors. Diphenylphosphoryl azide was prepared from diphenylphosphoryl chloride (Acros) [14]. Commercial reagents were used as received from Aldrich or Acros. Spectroscopic data were obtained in spectral grade solvents from Fisher and Acros. Deuterated chloroform and dimethylsulfoxide were from Cambridge Isotope Laboratories. The half-ester acid chloride of adipic acid was prepared previously [1] and pyrroles **15** and **16** were prepared as described previously [15, 16].

UV Measurements

Stock solutions of $3\times10^{-3}\,M$ of **1**–**8** were prepared by dissolving an appropriate amount of the desired pigment in 2 cm^3 $CHCl_3$. Next, a 0.1 cm^3 aliquot of the stock solution was diluted to 5 cm^3 (volumetric flask) with the specified organic solvent for UV-vis studies (Table 4). The final concentration of the solution was $\sim 2\times10^{-5}\,M$ in pigment. Up to four 5 cm^3 solutions of each pigment were prepared, as needed, in 5 cm^3 volumetric flasks. We carried out *Beer's* Law studies as described previously [1].

(4Z)-9-(5-Carboxamidopentanoyl)-2,3,7,8-tetraethyl-(10H)-dipyrrin-1-one (**1**, $C_{23}H_{33}N_3O_3$)

A solution of 50 mg (0.134 mmol) **11** in 20 cm^3 *DMF* was cooled with an ice-H_2O bath. To this was added 50 mg NH_4Cl (0.93 mmol), *DPPA* (1.0 cm^3, 4.6 mmol) in 5.0 cm^3 *DMF*, and triethylamine (2.0 cm^3, 14 mmol). The solution was protected by a drying tube of anhydrous $CaCl_2$ and stirred for 72 h, then poured into 100 cm^3 H_2O and extracted with CH_2Cl_2 (3×50 cm^3). The combined organic extracts were washed with H_2O (2×100 cm^3) and dried (Na_2SO_4). The solvent was removed by evaporation (roto-vap), and the residue was dissolved in CH_2Cl_2 and stored overnight at 0°C. The cold mixture was filtered, the filtrate was collected, and the solvent removed. The residue was purified by radial chromatography (6% CH_3OH–CH_2Cl_2 eluent) then crystallized from *n*-hexane-CH_2Cl_2 to give pure **1**. Yield 22 mg (52%); mp 194–195°C; IR (NaCl, film): $\bar{\nu} = 3296$, 2962, 2343, 1693, 1672, 1625, 1460, 1298 cm^{-1}; ^{1}H NMR ($CDCl_3$, 500 MHz): $\delta = 1.14$ (9H, m), 1.21 (3H, t, $J = 7.76$ Hz),

1.83 (2H, m), 1.99 (2H, m), 2.37 (2H, q, $J = 7.3$ Hz), 2.44 (2H, t, $J = 6.39$ Hz), 2.55 (4H, m), 2.81 (2H, q, $J = 7.76$ Hz), 2.92 (2H, t, $J = 8.67$ Hz), 5.82 (1H, brs), 6.01 (1H, s), 8.52 (1H, brs), 10.3 (1H, brs), 11.57 (1H, brs) ppm; ^{13}C NMR ($CDCl_3$, 125 MHz): $\delta = 14.1$, 15.4, 15.8, 16.8, 17.1, 17.3, 18, 18.6, 24.5, 25.7, 33.4, 40, 97.5, 128, 130.1, 131.1, 132.1, 133.1, 135, 147.9, 175.2, 178.5, 191.8 ppm.

(4Z)-9-(5-N-Methylcarboxamidopentanoyl)-2,3,7,8-tetraethyl-(10H)-dipyrrin-1-one
(**2**, $C_{24}H_{35}N_3O_3$)
As above for **1**, amide **2** was prepared from 10-oxosemirubin **11** and methylamine hydrochloride. Yield 37 mg (71%); mp 140–142°C; IR (NaCl, film): $\bar{\nu} = 3290$, 2933, 1684, 1640, 1461, 1278, 1160 cm^{-1}; ^{1}H NMR (*DMSO*-d_6, 500 MHz): $\delta = 1.06$ (3H, t, $J = 7.3$ Hz), 1.07 (3H, t, $J = 6.85$ Hz), 1.09 (3H, t, $J = 7.3$ Hz), 1.14 (3H, t, $J = 7.3$ Hz), 1.58 (4H, m), 2.11 (2H, t, $J = 6.39$ Hz), 2.29 (2H, q, $J = 7.3$ Hz), 2.54 (4H, m), 2.57 (3H, d, $J = 5$ Hz), 2.7 (2H, q, $J = 7.3$ Hz), 2.87 (2H, t, $J = 6.39$ Hz), 5.96 (1H, s), 7.67 (1H, brs), 10.34 (1H, brs), 10.65 (1H, brs) ppm; ^{13}C NMR (*DMSO*-d_6, 125 MHz): $\delta = 13.7$, 15.5, 15.7, 16.4, 2×16.5, 16.9, 17.9, 23.6, 25.1, 25.4, 35.3, 38.3, 96, 127.6, 128.8, 129.6, 132, 134, 147, 172.3, 172.4, 189.2 ppm.

(4Z)-9-(5-t-Butylcarboxamidopentanoyl)-2,3-dimethyl-7,8-diethyl-(10H)-dipyrrin-1-one
(**3**, $C_{25}H_{37}N_3O_3$)
As above for **1**, amide **3** was prepared from 10-oxosemirubin **13** and *tert*-butylamine. Yield 43 mg (75%); mp 182°C; IR (NaCl, film): $\bar{\nu} = 3319$, 2965, 1674, 1652, 1549, 1258, 1227, 1168, 731 cm^{-1}; ^{1}H NMR ($CDCl_3$, 500 MHz): $\delta = 1.14$ (3H, t, $J = 7.76$ Hz,), 1.18 (3H, t, $J = 7.76$ Hz), 1.32 (9H, s), 1.69 (2H, m), 1.75 (2H, m), 1.92 (3H, s), 2.11 (3H, s), 2.17 (2H, t, $J = 6.85$ Hz), 2.53 (2H, q, $J = 7.76$ Hz), 2.76 (2H, q, $J = 7.3$ Hz), 2.85 (2H, t, $J = 7.3$ Hz), 5.47 (1H, brs), 5.96 (1H, s), 9.01 (1H, brs), 9.68 (1H, brs) ppm; ^{13}C NMR (*DMSO*-d_6, 500 MHz): $\delta = 8.4$, 9.5, 15.7, 16.5, 17.9, 23.5, 25.3, 28.5, 36.1, 38.4, 49.7, 95.8, 126.7, 127.6, 128.8, 129.5, 132, 135.4, 141.7, 171.6, 172.7, 189.7 ppm.

(4Z)-9-(5-N,N-Diethylcarboxamidopentanoyl)-2,3-dimethyl-7,8-diethyl-(10H)-dipyrrin-1-one
(**4**, $C_{25}H_{37}N_3O_3$)
Following the procedure for **1**, 10-oxosemirubin **13** was converted to amide **4** with diethylamine. Yield 36 mg (72%); mp 134–135°C; IR (NaCl, film): $\bar{\nu} = 3276$, 2966, 2871, 1697, 1674, 1643, 1359, 1109, 730 cm^{-1}; ^{1}H NMR ($CDCl_3$, 300 MHz): $\delta = 1.1$ (3H, t, $J = 7.33$ Hz), 1.16 (6H, m), 1.22 (3H, t, $J = 6.95$ Hz), 1.78 (4H, m), 1.92 (3H, s), 2.11 (3H, s), 2.53 (4H, m), 2.8 (4H, m), 3.34 (2H, q, $J = 6.95$ Hz), 3.43 (2H, q, $J = 6.96$ Hz), 5.94 (1H, s), 9.31 (1H, brs), 10.0 (1H, brs) ppm; ^{13}C NMR (*DMSO*-d_6, 125 MHz): $\delta = 8.4$, 9.6, 13.1, 14.3, 15.7, 16.4, 16.5, 17.9, 23.6, 24.8, 32.1, 38.4, 41.3, 95.8, 126.7, 127.6, 128.9, 129.6, 132, 135.4, 141.7, 170.8, 172.7, 189.8 ppm.

(4Z)-9-(5-Carboxamidopentyl)-2,3,7,8-tetraethyl-(10H)-dipyrrin-1-one (**5**, $C_{23}H_{35}N_3O_2$)
Semirubin **9** was converted to its amide, as in the synthesis of **1** above. Yield 12 mg (32%); mp 246–247°C; IR (NaCl, film): $\bar{\nu} = 3349$, 2960, 2931, 1677, 1635, 1599, 1464, 1368, 1170, 682 cm^{-1}; ^{1}H NMR ($CDCl_3$, 300 MHz): $\delta = 1.1$ (3H, t, $J = 7.69$ Hz), 1.12 (3H, t, $J = 7.7$ Hz), 1.16 (3H, m), 1.19 (3H, t, $J = 7.69$ Hz), 1.43 (2H, m), 1.73 (4H, m), 2.39 (4H, m), 2.55 (4H, m), 2.75 (2H, m), 5.56 (1H, brs), 6.04 (1H, s), 8.91 (1H, brs), 9.83 (1H, brs) ppm; ^{13}C NMR (*DMSO*-d_6, 125 MHz): $\delta = 13.9$, 15.7, 16.3, 16.6, 16.7, 2×17.02, 17.5, 24.9, 25.5, 28.6, 30.1, 35, 97.7, 120.8, 121.1, 126.9, 128.4, 133.8, 146.7, 171.6, 174.3 ppm.

(4Z)-9-(5-N-Methylcarboxamidopentyl)-2,3,7,8-tetraethyl-(10H)-dipyrrin-1-one
(**6**, $C_{24}H_{37}N_3O_2$)
As above for **2**, semirubin **9** was converted to amide **6** with methylamine hydrochloride. Yield 30 mg (58%); mp 196–199°C; IR (NaCl, film): $\bar{\nu} = 3346$, 2931, 2962, 1673, 1659, 1643, 1564, 1169, 1012, 700 cm^{-1}; ^{1}H NMR (*DMSO*-d_6, 500 MHz): $\delta = 1.03$ (9H, m), 1.11 (3H, t, $J = 7.76$ Hz), 1.27 (4H, m),

1.52 (2H, m), 2.05 (2H, t, $J = 7.76$ Hz), 2.25 (2H, q, $J = 7.3$ Hz), 2.32 (2H, q, $J = 7.3$ Hz), 2.46 (6H, m), 2.54 (3H, d, $J = 4.56$ Hz), 5.91 (1H, s), 7.67 (1H, brs), 9.84 (1H, brs), 10.14 (1H, brs) ppm; ^{13}C NMR (*DMSO*-d_6, 125 MHz): $\delta = 13.9$, 15.8, 16.3, 16.6, 16.7, 2×17.0, 25.13, 25.4, 28.7, 30.1, 35.26, 97.7, 120.9, 121.1, 126.9, 128.4, 128.86, 133.7, 146.7, 171.6, 172.4 ppm.

(4Z)-9-(5-t-Butylcarboxamidopentyl)-2,3-dimethyl,7,8-diethyl-(10H)-dipyrrin-1-one
(**7**, $C_{25}H_{39}N_3O_2$)
Semirubin **10** was converted to amide **7** using the procedure above for the synthesis of **6**. Yield 44 mg (76%); mp 197–198°C; IR (NaCl, film): $\bar{\nu} = 3352$, 2960, 1674, 1644, 1560, 1548, 1468, 1363, 752 cm^{-1}; ^{1}H NMR ($CDCl_3$, 300 MHz): $\delta = 1.1$ (3H, t, $J = 7.69$ Hz), 1.16 (3H, t, $J = 7.32$ Hz), 1.3 (9H, s), 1.35 (4H, m), 1.62 (2H, m), 1.92 (3H, s), 2.06 (2H, t, $J = 7.69$ Hz), 2.12 (3H, s), 2.41 (2H, q, $J = 7.33$ Hz), 2.56 (2H, q, $J = 7.69$ Hz), 2.74 (2H, t, $J = 7.32$ Hz), 5.2 (1H, brs), 6.12 (1H, s), 10 (1H, brs), 11 (1H, brs) ppm; ^{13}C NMR (*DMSO*-d_6, 125 MHz): $\delta = 8.3$, 9.6, 16.6, 16.7, 17, 17.1, 25.3, 25.5, 28.5, 30.1, 36, 49.7, 97.6, 120.8, 121, 123.4, 128.5, 128.8, 133.6, 141.3, 171.6, 171.9 ppm.

(4Z)-9-(5-N,N-Diethylcarboxamidopentyl)-2,3-dimethyl,7,8-diethyl-(10H)-dipyrrin-1-one
(**8**, $C_{25}H_{39}N_3O_2$)
As above for **7**, semirubin **10** was converted to amide **8**. Yield 35 mg (60%); mp 116–118°C; IR (NaCl, film): $\bar{\nu} = 3353$, 2963, 2930, 1664, 1633, 1462, 1177, 692 cm^{-1}; ^{1}H NMR ($CDCl_3$, 300 MHz): $\delta = 1.05$ (3H, t, $J = 6.96$ Hz), 1.1 (3H, t, $J = 7.32$ Hz), 1.12 (3H, t, $J = 7.33$ Hz), 1.16 (3H, t, $J = 7.32$ Hz), 1.37 (2H, m), 1.68 (4H, m), 1.92 (3H, s), 2.11 (3H, s), 2.28 (2H, t, $J = 7.32$ Hz), 2.41 (2H, q, $J = 7.32$ Hz), 2.56 (2H, q, $J = 7.69$ Hz), 2.74 (2H, t, $J = 7.32$ Hz), 3.26 (2H, q, $J = 6.96$ Hz), 3.34 (2H, q, $J = 6.96$ Hz), 6.1 (1H, s), 10 (1H, brs), 10.85 (1H, brs) ppm; ^{13}C NMR (*DMSO*-d_6, 125 MHz): $\delta = 8.3$, 9.6, 13.1, 14.3, 16.6, 16.7, 17, 17.1, 24.8, 25.5, 28.7, 30.1, 32, 41, 41.3, 97.6, 120.8, 121, 123.4, 128.5, 128.8, 133.6, 141.3, 170.9, 171.9 ppm.

(4Z)-9-(5-Carboxypentyl)-2,3,7,8-tetraethyl-(10H)-dipyrrin-1-one (**9**, $C_{23}H_{34}N_2O_3$)
A solution of 125 mg (0.29 mmol) 10-oxosemirubin ester **12** in 100 cm^3 2-propanol was stirred while 200 mg (5.4 mmol) $NaBH_4$ were added in one portion. The mixture was heated at reflux for 3 h, and the hot mixture was poured into 200 cm^3 ice-H_2O and stirred while the solution was slowly acidified with 10% aq. HCl. The acidic solution was extracted with CH_2Cl_2 (3×75 cm^3), and the combined extracts were washed with H_2O (2×150 cm^3). After drying (Na_2SO_4), the solvent was removed by evaporation. The residue was dissolved in 100 cm^3 CH_2Cl_2 and 1.00 g (7.52 mmol) anhydrous $AlCl_3$ was added. The mixture was stirred at room temperature for 1.5 h and the mixture was poured into 200 cm^3 ice-H_2O and stirred for 30 min. The mixture was extracted with CH_2Cl_2 (3×75 cm^3), and the combined extracts were washed with H_2O (2×100 cm^3) and dried (Na_2SO_4). The solvent was removed by evaporation (roto-vap) and the residue was crystallized from *n*-hexane-CH_2Cl_2 to give pure semirubin **9**. Yield 80 mg (71%); mp 148–150°C; IR (NaCl, film): $\bar{\nu} = 3355$, 2934, 1710, 1661, 1464, 1274, 1059 cm^{-1}; ^{1}H NMR ($CDCl_3$, 500 MHz): $\delta = 1.1$ (3H, t, $J = 7.3$ Hz), 1.13 (3H, t, $J = 7.3$ Hz), 1.16 (3H, t, $J = 7.76$ Hz), 1.19 (3H, t, $J = 7.3$ Hz), 1.44 (2H, m), 1.63 (2H, m), 1.73 (2H, m), 2.37 (2H, q, $J = 7.3$ Hz), 2.4 (2H, q, $J = 7.3$ Hz), 2.48 (2H, t, $J = 6.39$ Hz), 2.54 (2H, q, $J = 7.3$ Hz), 2.55 (2H, q, $J = 7.3$ Hz), 2.72 (2H, t, $J = 6.39$ Hz), 7.26 (1H, s), 9 (1H, brs), 10.6 (1H, brs), 13.8 (1H, brs) ppm; ^{13}C NMR ($CDCl_3$, 75 MHz): $\delta = 14$, 15.9, 16.5, 16.8, 17, 17.2, 17.8, 17.9, 22.3, 23.7, 27.2, 29.3, 33.6, 101.3, 122, 122.4, 127.3, 128.6, 131.8, 135.9, 147.9, 174.5, 180.6 ppm.

(4Z)-9-(5-Carboxypentyl)-2,3-dimethyl-7,8-diethyl-(10H)-dipyrrin-1-one (**10**, $C_{21}H_{30}N_2O_3$)
Semirubin **10** was prepared from 10-oxosemirubin ester **14** as described above for **9** from **12**. Yield 100 mg (66%); mp 166–167°C; IR (NaCl, film): $\bar{\nu} = 3350$, 2963, 1707, 1662, 1462, 1176, 693 cm^{-1}; ^{1}H NMR ($CDCl_3$, 300 MHz): $\delta = 1.1$ (3H, t, $J = 7.69$ Hz), 1.16 (3H, t, $J = 7.33$ Hz), 1.43 (4H, m), 1.6 (2H, m), 1.73 (2H, m), 1.9 (3H, s), 2.11 (3H, s), 2.4 (2H, q, $J = 7.69$ Hz), 2.49 (3H, m), 2.58 (2H, q, $J = 7.69$ Hz), 2.72 (2H, t, $J = 6.23$ Hz), 6.11 (1H, s), 8.98 (1H, brs), 10.56 (1H, brs), 13.92

(1H, brs) ppm; ^{13}C NMR ($CDCl_3$, 75 MHz): $\delta = 8.2$, 9.8, 16.5, 16.9, 17.2, 17.8, 21.2, 22.8, 26.4, 28.9, 32.9, 101.1, 121.9, 122.4, 123.6, 128.6, 131.7, 135.8, 142.2, 174.7, 180.8 ppm.

(4Z)-9-(5-Carboxypentanoyl)-2,3,7,8-tetraethyl-(10H)-dipyrrin-1-one (**11**, $C_{23}H_{32}N_2O_4$)
To a solution of 150 mg (0.35 mmol) 10-oxosemirubin ester **12** in 100 cm^3 *THF* were added 30 cm^3 2 *M* aq. NaOH, and the solution was heated to reflux for 3 h. The warm solution was poured into 200 cm^3 ice-H_2O and acidified slowly with 10% aq. HCl. The acidified solution was extracted with 3×50 cm^3 CH_2Cl_2, then washed with H_2O (2×100 cm^3) and dried (Na_2SO_4). The organic solvent was removed by evaporation (roto-vap) and the residue was crystallized from *n*-hexane-CH_2Cl_2 to give pure **11**. Yield 124 mg (89%); mp 142–144°C; IR (NaCl, film): $\bar{\nu} = 3272$, 2967, 1698, 1683, 1652, 1458, 1267, 1164, 434 cm^{-1}; ^{1}H NMR ($CDCl_3$, 300 MHz): $\delta = 1.17$ (12H, m), 1.8 (2H, m), 1.94 (2H, m), 2.4 (2H, q, $J = 7.69$ Hz), 2.55 (4H, m), 2.8 (2H, q, $J = 7.69$ Hz), 2.86 (4H, m), 6.1 (1H, s), 9.2 (1H, brs), 10.8 (1H, brs), 12.9 (1H, brs) ppm; ^{13}C NMR ($CDCl_3$, 75 MHz): $\delta = 14$, 15.6, 15.8, 16.8, 17, 17.4, 18, 18.6, 23.8, 25.1, 33.7, 39.6, 99.1, 127.7, 130.4, 131.4, 132.4, 133.5, 134.5, 148.3, 175.7, 180.4, 190.6 ppm.

(4Z)-9-(5-Carboethoxypentanoyl)-2,3,7,8-tetraethyl-(10H)-dipyrrin-1-one (**12**, $C_{25}H_{36}N_2O_4$)
A suspension of 3 g (22.5 mmol) anhydrous $AlCl_3$ in 100 cm^3 CH_2Cl_2 in a 500 cm^3 round bottom flask equipped with a drying tube ($CaCl_2$) was cooled to 0°C with an ice bath. To the mixture was added 1.33 g (0.753 mmol) freshly-distilled 5-carboethoxypentanoyl chloride (prepared from reaction of the half-ester [**1**]) in one portion. The mixture was stirred for an additional 10 min, then, 400 mg (1.47 mmol) dipyrrinone **15** in 150 cm^3 CH_2Cl_2 were added in one portion to the mixture. The mixture was stirred at room temperature for 15 h, then poured into 300 cm^3 ice-H_2O and stirred for 30 min. The solution was extracted with CH_2Cl_2 (3×75 cm^3) and the combined extracts were washed with H_2O (3×100 cm^3). After drying (Na_2SO_4), evaporation of the solvent left a residue that was subjected to radial chromatography using CH_2Cl_2–CH_3OH (98:2, *v*/*v*) as eluent. The solid obtained by chromatography was recrystallized from *n*-hexane-CH_2Cl_2 to give pure **12**. Yield 377 mg (60%); mp 109–110°C; IR (NaCl, film): $\bar{\nu} = 3311$, 2967, 2933, 1735, 1670, 1653, 1263, 1111 cm^{-1}; ^{1}H NMR ($CDCl_3$, 300 MHz): $\delta = 1.12$ (3H, t, $J = 7.69$ Hz), 1.2 (9H, m), 1.25 (3H, t, $J = 6.96$ Hz), 2.37 (5H, m), 2.53 (8H, m), 2.75 (2H, q, $J = 7.69$ Hz), 2.85 (2H, t, $J = 6.96$ Hz), 4.12 (2H, q, $J = 6.95$ Hz), 5.96 (1H, s), 8.66 (1H, brs), 9.37 (1H, brs) ppm; ^{13}C NMR ($CDCl_3$, 75 MHz): $\delta = 13.8$, 14.5, 15.4, 16.3, 16.4, 17.2, 17.6, 18, 18.9, 24.4, 25, 34.5, 39.2, 60.6, 96.8, 129, 130, 130.5, 132.9, 133.7, 136, 147.5, 173.1, 173.8, 189.7 ppm.

(4Z)-9-(5-Carboxypentanoyl)-2,3-dimethyl-7,8-diethyl-(10H)-dipyrrin-1-one (**13**, $C_{21}H_{28}N_2O_4$)
10-Oxosemirubin **13** was prepared by saponification of its ester, as described above for **11** from **12**. Yield 104 mg (89%); mp 151–153°C; IR (NaCl, film): $\bar{\nu} = 3272$, 2965, 1699, 1674, 1652, 1435, 1264, 1170, 757 cm^{-1}; ^{1}H NMR ($CDCl_3$, 300 MHz): $\delta = 1.14$ (6H, t, $J = 7.32$ Hz), 1.814 (2H, m), 1.9 (2H, m), 1.94 (3H, s), 2.14 (3H, s), 2.56 (5H, m), 2.81 (5H, m), 6.1 (1H, s), 9.17 (1H, brs), 10.75 (1H, brs), 12.7 (1H, brs) ppm; ^{13}C NMR ($CDCl_3$, 125 MHz): $\delta = 8.6$, 10.1, 15.4, 16.7, 17.3, 18.6, 23.3, 25.4, 33.1, 39.9, 99, 127.5, 127.5, 130.3, 131.6, 134.7, 134.9, 143, 176, 180.7, 190.9 ppm.

(4Z)-9-(5-Carboethoxypentanoyl)-2,3-dimethyl-7,8-diethyl-(10H)-dipyrrin-1-one
(**14**, $C_{23}H_{32}N_2O_4$)
Analog **14** was prepared from dipyrrinone **16** as outlined above for **12** from **15**. Yield 744 mg (76%); mp 118°C; IR (NaCl, film): $\bar{\nu} = 3319$, 2965, 1735, 1672, 1649, 1438, 1258, 1172 cm^{-1}; ^{1}H NMR ($CDCl_3$, 300 MHz): $\delta = 1.68$ (3H, t, $J = 7.7$ Hz), 1.22 (2H, m), 1.24 (3H, t, $J = 7.3$ Hz), 1.73 (4H, m), 1.93 (3H, s), 2.11 (3H, s), 2.34 (2H, t, $J = 6.6$ Hz), 2.53 (2H, q, $J = 7.3$Hz), 2.76 (2H, q, $J = 7.3$ Hz), 2.89 (3H, t, $J = 6.6$ Hz), 4.12 (2H, q, $J = 7.3$ Hz), 5.97 (1H, s), 9.47 (1H, brs) ppm; ^{13}C NMR ($CDCl_3$, 125 MHz): $\delta = 8.6$, 9.9, 14.2, 16, 16.4, 17.2, 18.6, 23.9, 24.7, 34.2, 38.9, 60.3, 97, 128, 128.6, 130.2, 130.4, 132.7, 135.9, 142.1, 173.6, 174, 189.7 ppm.

X-Ray Structure and Solution

Crystals of **2** were grown by vapor diffusion of diethyl ether into a solution of CH_2Cl_2. A crystal (approximate dimensions $0.31 \times 0.25 \times 0.02\,mm^3$) was placed onto the tip of a 0.1 mm diameter glass capillary and mounted on a Bruker SMART Apex system for data collection at 100(2) K. A preliminary set of cell constants was calculated from reflections harvested from 3 sets of 20 frames. These initial sets of frames were oriented such that orthogonal wedges of reciprocal space were surveyed (final orientation matrices determined from global least-squares refinement of 5809 reflections). The data collection was carried out using MoKα radiation (0.71073 Å graphite monochromator) with a frame time of 20 s and a detector distance of 4.94 cm. A randomly oriented region of reciprocal space was surveyed to the extent of 2 hemispheres and to a resolution of 0.66 Å. Four major sections of frames were collected with 0.3° steps in ω at 600 different ϕ settings and a detector position of 36° in 2θ. The intensity data were corrected for absorption and decay (SADABS) [23]. Final cell constants were calculated from the *xyz* centroids of strong reflections from the actual data collection after integration (SAINT 6.45, 2003) [24]. Crystal data and refinement information for **2** may be found in Table 5.

The structure was solved and refined using SHELXL-97 [25]. The triclinic space group P-1 was determined based on systematic absences and intensity statistics. A direct-methods solution was

Table 5. Crystal data and structure refinement for 10-oxo-[6]-semirubin *N*-methylamide (**2**)

Empirical formula	$2 \times C_{24}H_{35}N_3O_3$
Formula weight	2×413.55
Crystallized from	diethyl ether/CH_2Cl_2
Temperature/K	100(2)
Wavelength	0.71073 Å
Crystal size	$0.31 \times 0.25 \times 0.02\,mm^3$
Crystal system	Triclinic
Space group	*P*-1
Z	2
Unit cell dimensions	$a = 12.6904(10)$ Å $\alpha = 100.566(2)°$ $b = 13.5722(11)$ Å $\beta = 94.706(2)°$ $c = 14.0802(11)$ Å $\gamma = 105.138(2)°$
Volume/Å^3	2279.6(3)
Density (calculated)/Mg/m^{-3}	1.204
Absorption coefficient/mm^{-1}	0.080
F(000)	894
Crystal habit and color	yellow plates
Theta range for data collection/°	1.59 to 32.29
Index ranges	$-19 \le h \le 19,\ -20 \le k \le 20,\ -20 \le l \le 21$
Reflections collected	40573
Independent reflections	15975 [*R*(int) = 0.0919]
Completeness to theta = 32.29°/%	98.6
Absorption correction	SADABS
Max. and min. transmission	0.9983 and 0.9759
Refinement method	Full-matrix least-squares on F^2
Data/restraints/parameters	15975/0/551
Goodness-of-fit on F^2	0.934
Final *R* indices [$I > \sigma(I)$]	$R^1 = 0.0671$, $wR^2 = 0.1312$
R indices (all data)	$R^1 = 0.1689$, $wR^2 = 0.1676$
Largest diff. peak and hole/e.Å^{-3}	0.628 and −0.451

calculated which provided most non-hydrogen atoms from the E-map. Full-matrix least squares/ difference *Fourier* cycles were performed which located the remaining non-hydrogen atoms. All non-hydrogen atoms were refined with anisotropic displacement parameters unless stated otherwise. The data were corrected for absorption using an empirical model derived from psi scans. Hydrogen atom positions were placed in ideal positions and refined as riding atoms with relative isotropic displacement parameters (a C–H distance fixed at 0.96 Å and a thermal parameter 1.2 times the host carbon atom). Tables of atomic coordinates, bond lengths and angles, anisotropic displacement parameters, hydrogen coordinates, and isotropic displacement parameters have been deposited at the Cambridge Crystallographic Data Centre, CCDC No. 269740 for **2**.

Acknowledgements

We thank the U.S. National Institutes of Health (HD-17779) for generous support. We also thank the National Science Foundation (CHE-0226402) for providing funding to purchase the X-ray diffractometer used in this work. *NTS* thanks the National Institutes of Health for fellowship support.

References

[1] Huggins MT, Lightner DA (2000) J Org Chem **65**: 6001
[2] Huggins MT, Lightner DA (2001) Tetrahedron **57**: 2279
[3] Falk H (1989) The Chemistry of Linear Oligopyrroles and Bile Pigments. Springer-Verlag, Wien
[4] Chowdhury JR, Wolkoff AW, Chowdhury NR, Arias IM (2001) Hereditary Jaundice and Disorders of Bilirubin Metabolism. In: Scriver CF, Beaudet AL, Sly WS, Valle D (eds) The Metabolic and Molecular Bases of Inherited Disease, chap 125, McGraw-Hill, New York, pp 3063–3101
[5] a) Sheldrick WS (1983) Israel J Chem **23**: 155; b) Sheldrick WS (1976) J Chem Soc Perkin **2**: 1457; c) Bonnett R, Davies JE, Hursthouse NB, Sheldrick GM (1978) Proc R Soc London, Ser B **202**: 249; d) LeBas G, Allegret A, Mauguen Y, DeRango C, Bailly M (1980) Acta Crystallogr Sect B **B36**: 3007; e) Becker W, Sheldrick WS (1978) Acta Crystallogr Sect B **B34**: 1298
[6] Person RV, Peterson BR, Lightner DA (1994) J Am Chem Soc **116**: 42
[7] Nogales D, Lightner DA (1995) J Biol Chem **270**: 73
[8] Falk H, Grubmayr K, Höllbacher G, Hofer O, Leodolter A, Neufingerl F, Ribó JM (1977) Monatsh Chem **108**: 1113
[9] Brower JO, Huggins MT, Boiadjiev SE, Lightner DA (2000) Monatsh Chem **131**: 1047
[10] Galliani G, Monti D, Speranza G, Manitto P (1984) Tetrahedron Lett **25**: 6037
[11] Chen Q, Huggins MT, Lightner DA, Norona W, McDonagh AF (1999) J Am Chem Soc **121**: 9253
[12] Boiadjiev SE, Person RV, Lightner DA (1993) Tetrahedron Asymm **4**: 491
[13] Boiadjiev SE, Anstine DT, Lightner DA (1994) Tetrahedron Asymm **5**: 1945
[14] Shioiri T, Ninomiya K, Yamada S (1972) J Am Chem Soc **94**: 6203
[15] Bonnett R, Buckley DG, Hamzetesh D (1981) J Chem Soc Perkin I 322
[16] Huggins MT, Lightner DA (2000) Tetrahedron **56**: 1797
[17] Nogales DF, Ma J-S, Lightner DA (1993) Tetrahedron **49**: 2361
[18] Huggins MT, Lightner DA (2001) Monatsh Chem **132**: 203
[19] a) Boiadjiev SE, Anstine DT, Lightner DA (1995) J Am Chem Soc **117**: 8727; b) Boiadjiev SE, Anstine DT, Maverick E, Lightner DA (1995) Tetrahedron Asymm **6**: 2253
[20] a) Cullen DL, Black PS, Meyer EF, Lightner DA, Quistad GB, Pak C-S (1977) Tetrahedron **33**: 477; b) Cullen DL, Pèpe G, Meyer EF Jr, Falk H, Grubmayr K (1979) J Chem Soc Perkin II 999

[21] Molecular mechanics and dynamics calculations employed to find the global energy minimum conformations of **1**–**6** were run on an SGI Octane workstation using vers 7.0 of the Sybyl forcefield as described in refs [6] and [12]; the Ball and Stick drawings were created from the atomic coordinates using *Müller* and *Falk's* "Ball and Stick" program for the Macintosh (http://www.orc.uni-Linz.ac.at/mueller/ball_and_stick.shtml)
[22] Sheldrick WS, Borkenstein A, Blacha-Puller M, Gossauer A (1977) Acta Crystallogr **B33**: 3625
[23] Blessing R (1995) Acta Crystallogr **A51**: 33
[24] SAINT V6.45, Bruker Analytical X-ray Systems, Madison, WI, USA
[25] SHELXTL-Plus V5.10, Bruker Analytical X-ray Systems, Madison, WI, USA